Liquid alkali metals at the melting point: Structural and dynamical properties

Umberto Balucani
Istituto di Elettronica Quantistica, Consiglio Nazionale delle Ricerche, I-50127 Firenze, Italy

Alessandro Torcini
Dipartimento di Fisica, Università di Firenze, I-50125 Firenze, Italy

Renzo Vallauri
Dipartimento di Fisica, Università di Trento, I-38050 Povo, Italy
(Received 7 May 1992; revised manuscript received 6 October 1992)

In this paper we report the results of a comprehensive simulation study of the structural and dynamical properties of liquid Na, K, Rb, and Cs near the melting point. An important consequence of this investigation is that both the equilibrium and the time-dependent correlations can be cast in a properly scaled form, which is to a very good approximation the same for all the alkali metals. In particular, for liquid Cs the simulation findings for the dynamic structure factor are found to be in excellent agreement with the inelastic-neutron-scattering data recently reported. Finally, the analysis is extended to the two main transport properties, the diffusion and the shear-viscosity coefficients. The simulation results compare satisfactorily with the actual experimental findings and confirm the validity of the simplified mode-coupling approaches recently proposed for these two quantities.

I. INTRODUCTION

The properties of monatomic liquid metals have always attracted several experimental investigations, both for their intrinsic interest as well as for the understanding of the structural and dynamical features of simple liquids.[1] A recent example is the report of new accurate neutron-scattering measurements of the dynamical structure factor of liquid caesium slightly above the melting point.[2] The analysis of these data and the comparison with similar results in other liquid alkali metals naturally raises the question of ascertaining possible common features in this important class of systems. For instance, the Cs data of Ref. 2 give clear evidence for density fluctuations propagating with wave vectors substantially larger than those typical of the hydrodynamic regime; this feature, absent in the typical Lennard-Jones liquids, is instead completely consistent with previous findings in liquid rubidium.[3]

This and several other analogies in the structural and dynamical behavior of liquid alkali metals indicate the possible existence of a potential model whose functional form is universal for all these elements under appropriate scaling. Several attempts to verify the validity of a "corresponding states law" have indeed been made.[4–7] A difficulty is that the effective pair potential $v(r)$ between the ions is density dependent; moreover, the parameters entering $v(r)$ are often determined by a fitting procedure on the properties of the corresponding solid. As a consequence, "natural" length and energy scales by which $v(r)$ can be cast into a universal form are not apparent *a priori*. As in the Lennard-Jones case, one may choose as proper scaling quantities the energy ε of the main potential well of $v(r)$ and the minimum distance σ where the potential vanishes. This procedure was actually suggested in Ref. 4, where the scaled version of the potential implemented by Price, Singwi, and Tosi[8] was found to reproduce fairly well several *static* properties for Na, K, and Rb. At that time, the accuracy of the experimental data was not good enough to make more definite assessments about scaling behavior. Nowadays, a more complete analysis of the problem including both structural and dynamical features appears to be possible, and this is one of the main topics addressed in the present paper.

A second point of interest in the recent findings is the possibility of providing a realistic benchmark for the non-phenomenological theories of the liquid state dynamics as developed in the last decade.[9] This test appears to be particularly enlightening in view of the simplifications which have recently been proposed[10–12] in the formal structure of the kinetic equations, making several properties amenable to rather straightforward calculations.

Computer experiments are obviously helpful to elucidate both the aforementioned aspects. In the following we shall report a series of molecular-dynamics (MD) simulations for several liquid alkali metals (Na, K, Rb, and Cs) near melting, by which the main static and dynamical correlation functions can be deduced.

The format of the present paper is as follows. In Sec. II we specify the potential model (essentially the one developed in Ref. 8), discuss the first "evidences" for a scaling behavior, and report the MD results for the main structural quantities of the liquids under consideration. Section III deals with an important set of dynamical quantities, namely, the intermediate scattering function $F(k,t)$ and its self part $F_S(k,t)$. In particular, here the simulation results for the dynamic structure factor $S(k,\omega)$ in liquid Cs are compared with the corresponding neutron data of Ref. 2. Also, the validity of the scaling for different alkali metals is carefully checked even for these time-dependent quantities. Finally, Sec. IV is entirely devoted to the analysis of the two main transport properties, namely, the diffusion and the shear-viscosity

coefficients. Here the MD findings for the corresponding Green-Kubo integrands are compared with the theoretical predictions based on a simplified mode-coupling approach. The values of the transport coefficients are eventually compared with the available experimental data for the alkali metals near the melting point.

II. INTERACTION POTENTIAL AND STRUCTURAL QUANTITIES

A first evidence that alkali metals may be expected to show a universal behavior is provided by the recognition that near the melting point the static structure factors $S(k)$ for Na, K, Rb, and Cs are almost coincident when reported as a function of the scaled unit k/k_m, where k_m denotes the position of the main peak of $S(k)$ in each system. Using both x-ray- and neutron-diffraction data, the structure factor can be scaled even by adopting slightly different recipes.[4,5,7,13]

This property suggests that an effective ion-ion interaction potential should also have a simple scaling behavior. On the other hand, a physically based potential model for metals has to account for the screening effect of the conducting electrons on the sheer electrostatic interaction. In particular, the model proposed by Price, Singwi, and Tosi[8] reads

$$v(r)=\frac{(Ze)^2}{r}\left[1-\frac{2}{\pi}\int_0^\infty dq\, G(q)\frac{\sin(qr)}{q}\right], \qquad (2.1)$$

where Ze is the ionic charge and $G(q)$ is related to the Fourier transform of an empty core pseudopotential properly modified to include the above-mentioned screening effect. The model parameters present in $G(q)$ turn out to be dependent on the number density $n=N/V$. In practice, the form of $G(q)$ proposed in Ref. 8 is such that no natural lengths and/or energies are apparent in $v(r)$, so that a possible scaling behavior can only be tested *a posteriori*. Using the parameters reported in Ref. 8 we have evaluated $v(r)$ for Na, K, Rb, and Cs at the thermodynamic conditions near the respective melting points (for details see Table I). Broadly speaking, all these potentials show a repulsive portion (noticeably softer than the corresponding one for the Lennard-Jones case) down to a negative minimum denoted by $-\varepsilon$; this first potential well is then followed by damped oscillations of the Friedel form. The quantities σ and ε may tentatively be taken as length and energy scaling parameters, as proposed by Mountain.[4] In other words, if we plot $v(r)/\varepsilon$ vs the reduced length $r^*=r/\sigma$, the function

$$v^*(r^*)=\frac{1}{\varepsilon}v\left[\frac{r}{\sigma}\right] \qquad (2.2)$$

should appear virtually the same for all the elements. Indeed, it is found that the scaling behavior expressed in Eq. (2.2) is well reproduced, Na being the element for which the largest deviations occur.[13] We have then proceeded to the calculation of the structural properties by using computer simulation techniques. Since we are also interested in the dynamical properties we have chosen the molecular-dynamics method; in particular, a system of $N=250$ or 432 particles interacting through the Price potential has been considered in a cubic box and the motion of the particles within a microcanonical ensemble has been followed using standard MD programs, $\delta t=10$ fs being the integration time step. The static (and subsequently dynamical) quantities have been obtained by averaging over runs as long as 120 000 time steps. These comparatively long simulations provide accurate results for all the properties under investigation, in particular, for those connected with dynamical quantities having a collective character. For example, the evaluation of the viscosity coefficient requires the computation of nondiagonal elements of the stress tensor: the associated correlation functions, besides being relatively long lived, show an anisotropic behavior which washes out only for long simulation runs.[14]

First of all, we have evaluated the radial distribution functions $g(r)$ and the static structure factors

$$S(k)=1+n\int d\mathbf{r}[g(r)-1]\exp(i\mathbf{k}\cdot\mathbf{r}) . \qquad (2.3)$$

In order to check the reliability of the Price potential for all the systems, $S(k)$ has to be compared with the available data obtained both by x-ray and neutron diffraction. Care must be taken in extending the radial distribution function beyond the accessible limit, imposed by the finite size of our simulation cell (i.e., half of the box length L). The extrapolation has been achieved by fitting the simulation data beyond the distance $r_0=1.128\sigma$ to a functional form

$$g(r)=[g(r_0)-1]e^{-B(r-r_0)}\cos[C(r-r_0)]+1 , \qquad (2.4)$$

where B,C are suitable parameters. This procedure yields an accurate Fourier transform since the integral in Eq. (2.3) can be extended up to distances where $g(r)$ becomes as close to one as desired. The results for the different liquid metals are reported in Fig. 1, along with the experimental data (both x-ray and neutron); the agreement is clearly very good. In Fig. 2, the MD data for the various radial distribution functions are shown as a function of reduced units $r^*=r/\sigma$. They appear to fall onto a universal curve for all the considered systems. Therefore, it is straightforward to show from Eq. (2.3)

TABLE I. Thermodynamic state points where the simulations have been performed and the correspondent parameters of the Price potential. n and T are the number density and the temperature expressed in units of Å^{-3} and K, respectively. σ (in units of Å) indicates the position of the first zero of the potential, ε (in units of K) the value of the main potential well, and $\tau=(m\sigma^2/\varepsilon)^{-1/2}$ (in units of ps) the time scale adopted to characterize the dynamical features.

	Na	K	Rb	Cs
n	0.024 29	0.012 84	0.010 45	0.008 3
T	376	343	318	308
σ	3.328	4.115	4.408	4.761
ε	445.60	420.99	402.20	386.49
τ	0.829	1.376	2.229	3.061

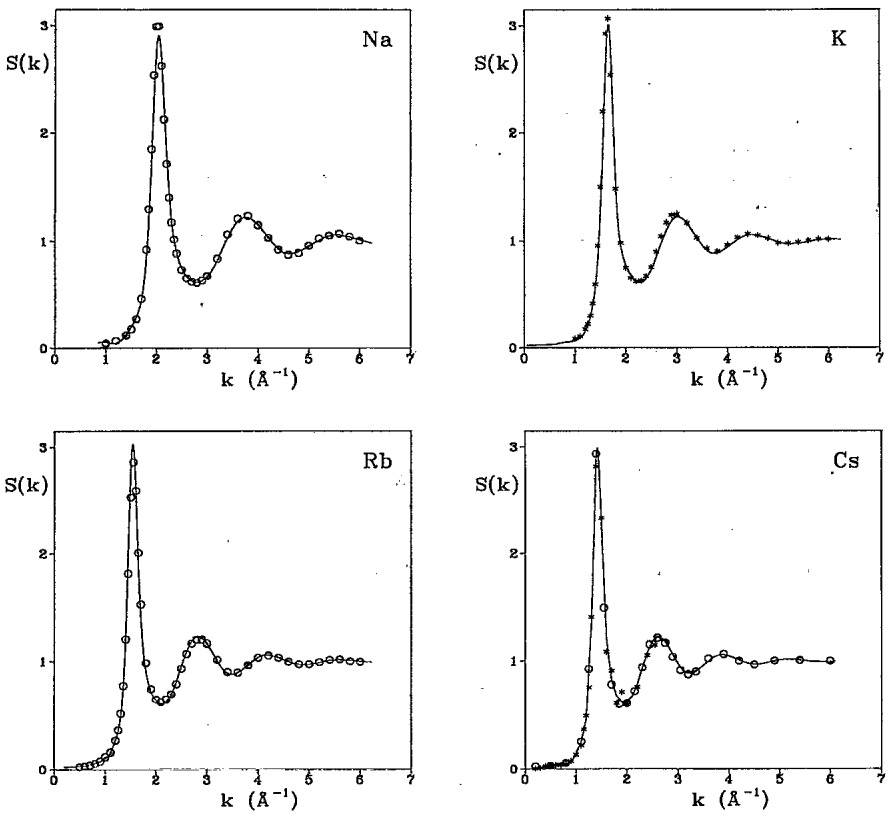

FIG. 1. Static structure factors for liquid Na, K, Rb, and Cs, at the thermodynamic points reported in Table I. The solid line is our MD findings. The asterisk refers to the neutron-diffraction data (reported in Ref. 2 for Cs and in Ref. 17 for Rb) and the circles to the x-ray data reported in Ref. 17.

that the structure factors also present a "universal" form if they are reported in terms of the reduced wave vectors $k^*=k\sigma$ at the same reduced density $n^*=n\sigma^3$. This behavior is also well reproduced by the experimental data within a few percent tolerance. Besides providing clear evidence of the reliability of the Price model for the alkali metals, these results give additional support to the idea that the real interaction potential can be cast into a universal form. Both these conclusions are now possible in view of the higher accuracy of the experimental data. Strictly speaking, on the basis of the corresponding states law, a property would be expected to scale exactly for systems at equal reduced temperature ($T^*=k_BT/\varepsilon$) and density ($n^*=N/V\sigma^3$). As a matter of fact, while the reduced densities of the examined alkali metals, at their respective melting point, are very much the same (ranging from $n^*=0.8952$ in K to $n^*=0.8957$ in Cs), the reduced temperatures are slightly different (ranging from $T^*=0.79$ in Rb to $T^*=0.84$ in Na). Thus, the observed scaling behavior points out the fact that the structure is not influenced very much by small temperature differences, a result already known for other model systems (e.g., Lennard-Jones fluids).

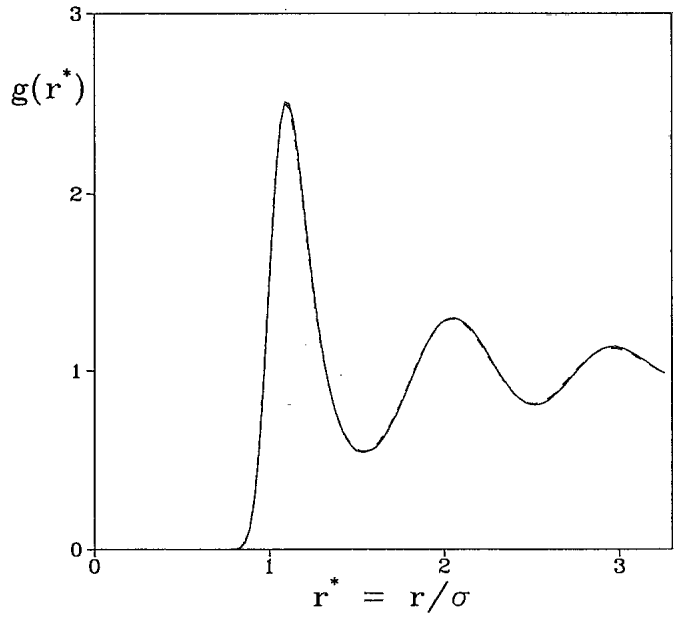

FIG. 2. The radial distribution function $g(r)$ for the liquid alkali metals Na, K, Rb, and Cs near the melting point, reported as a function of the reduced length $r^*=r/\sigma$. The solid line refers to Cs and the dashed one to Na; the results for K and Rb lie in between and are undiscernible on the scale of the graph.

III. INTERMEDIATE SCATTERING FUNCTIONS

Dealing with the dynamical properties of liquid alkali metals we will be concerned with the two main topics. First, we will compare the MD results obtained for liquid Cs with the recent neutron-scattering data of Ref. 2. Second, we will ascertain the validity of a scaling assumption even for the dynamics.

In our MD simulations, the intermediate scattering function $F(k,t)$ of liquid Cs has been evaluated at the same density and temperature as in the real experiment of Ref. 2. The components of the wave vectors $\mathbf{k}=(k_x,k_y,k_z)$ are chosen of the form $k_\alpha=(2\pi/L)n_\alpha$, where n_α is a positive integer and L is the length of the simulation box. Thus, the minimum wave vector ex-

plored is obtained for $N=432$, where $L=37.34$ Å and $k_{\min}=0.168$ Å^{-1}. To improve the statistics, for a given value of $|\mathbf{k}|$ the indexes are rotated along the three axes and a final average over the distinct orientations of $\mathbf{k}$ is performed. In units of Δt, liquid Cs requires simulation runs distinctly longer than the other alkali metals to obtain a comparable accuracy. This feature is consistent with the increase of the typical time scale $\tau=(m\sigma^2/\varepsilon)^{1/2}$ from Na to Cs (see Table I).

The features of $F(k,t)$ at different wave vectors are found to be qualitatively similar to those reported by Rahman[15] for liquid rubidium; in particular, even liquid Cs is found to support well-defined density oscillations beyond the hydrodynamic region. The dynamic structure factors $S(k,\omega)$ at different wave vectors are readily obtained from a Fourier transform of the corresponding $F(k,t)$. In Fig. 3 some typical MD results are reported along with the corresponding neutron-scattering data of Ref. 2. The agreement is clearly rather good, indicating that the potential model of Price, Singwi, and Tosi[8] is sufficiently realistic even for the dynamical features of liquid Cs. On the other hand, the gross features of $S(k,\omega)$ are rather unsensitive to the detailed form of $v(r)$. During the completion of this work we became aware of analogous MD simulations for liquid Cs by Kambayashi and Kahl.[16] Although these authors used a slightly different form for $G(q)$ in Eq. (2.1), the quality of the comparison between their MD results and the experimental data of Ref. 2 appears to be similar to the one reported in the present work.

The presence of well-defined density modes at relatively large wave vectors appears to be peculiar to liquid alkali metals near the melting point. Broadly speaking, this feature can be traced back to the comparatively soft repulsive potential and to its rather symmetrical shape around the main minimum.[18] These analogies in the dynamics of different systems can be made more specific if we consider a particular potential model. For example, in the case of the Price potential we have shown that σ and ε are the proper parameters to scale structural properties from one alkali element to another. For the dynamical properties we clearly need an analogous time unit; simple dimensional arguments indicate that such time unit is provided by the aforementioned quantity $\tau=(m\sigma^2/\varepsilon)^{1/2}$.

To ascertain the validity of this scaling for the dynamics, in Fig. 4 we report our MD data for the inelastic peak frequencies of $S(k,\omega)$ properly scaled for the various alkali metals. As is apparent, the consistency among these different dispersion relations is excellent. Also, the inelastic peak is found to disappear beyond a reduced wave vector $k_0^*=k_0\sigma$, which is approximately the same for all the elements; the data indicate that $k_0^*\simeq 5.2$, roughly $\frac{3}{4}$ of the wave vector $k_m^*\simeq 6.8$ where the structure factors $S(k^*)$ attain their main maximum. To make a closer contact between these simulation findings and the data of real measurements, in Fig. 4 we have also reported some scaled peak frequencies deduced from the inelastic-neutron-scattering experiments in liquid Rb (Ref. 3) and in liquid Cs.[2] This comparison parallels the one performed in Fig. 1 for $S(k)$. The good agreement between MD data and experimental findings points out the validity of the scaling even for the real systems.

As expected, a similar universal behavior is found even

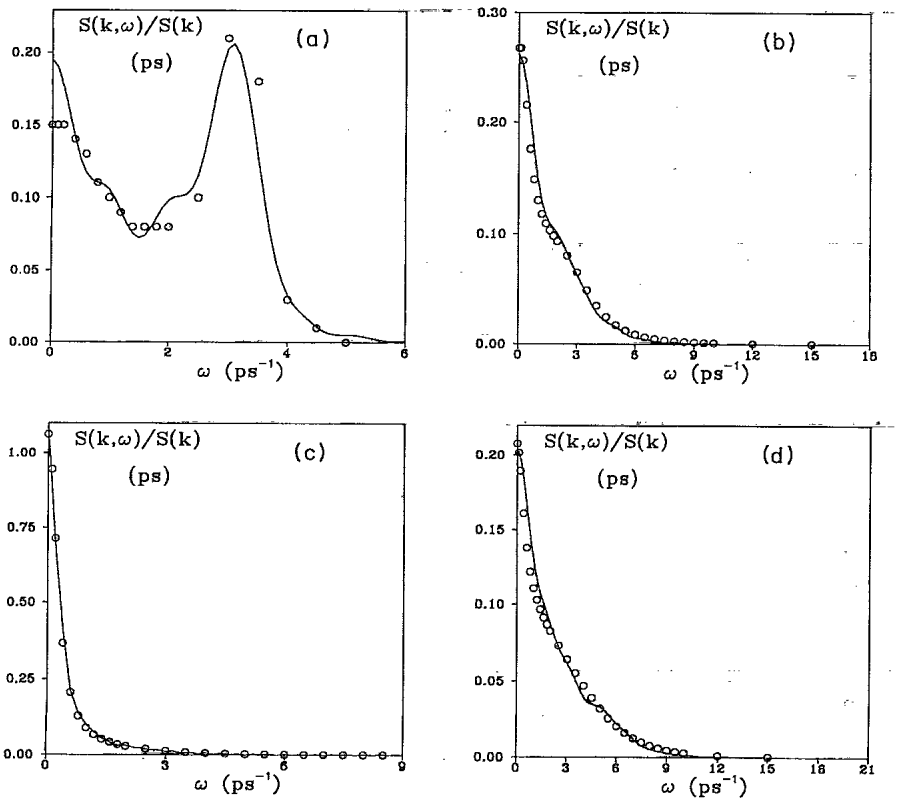

FIG. 3. Dynamic structure factors of liquid Cs at 308 K for several wave vectors k: (a) 0.3 Å^{-1}, (b) 1.2 Å^{-1}, (c) 1.4 Å^{-1}, (d) 1.8 Å^{-1}. Solid line: our MD findings. Circles: neutron-scattering data of Ref. 2.

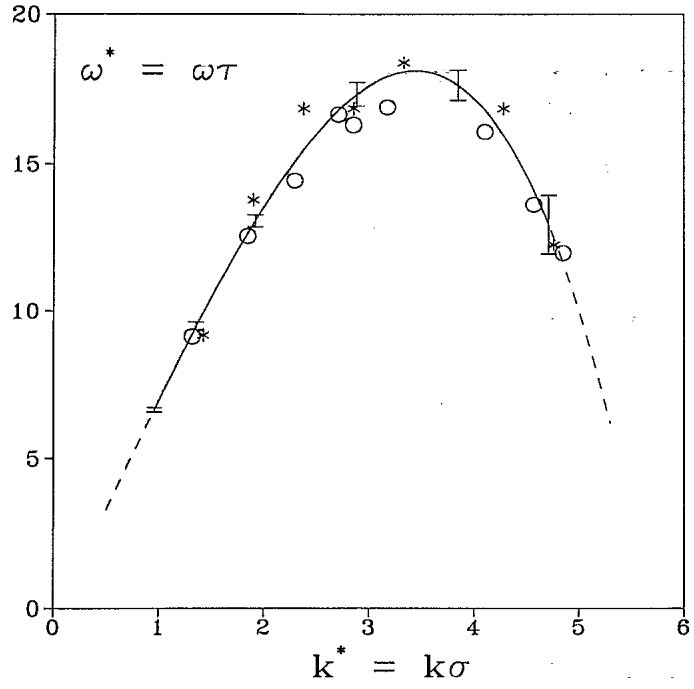

FIG. 4. Dispersion relation of the scaled peak frequencies of the dynamic structure factor for liquid alkali metals. The solid line represents the average of our MD results; the error bars give an idea of the maximum discrepancies observed among the different elements. The symbols refer to the properly scaled neutron data in Rb (circles, Ref. 3) and Cs (asterisks, Ref. 2).

for the detailed time evolution of the scattering functions of the examined alkali metals at different reduced wave vectors. In Figs. 5(a) and 5(b) we report such a comparison among the various $F(k^*,t^*)$, where $t^*=t/\tau$. The two reduced wave vectors have been chosen to illustrate different physical situations. In particular, the first one ($k^*=1.92$) probes a wave-vector region supporting well-defined density oscillations. The latter are instead absent for $k^*=6.86>k_0^*$: since this reduced wave vector is quite near k_m^*, one expects a pronounced "de Gennes" slowing down of $F(k^*,t^*)$, which is indeed observed.

Broadly speaking, all the main qualitative features of these intermediate scattering functions can be explained within a simple viscoelastic model in which the second-order memory function of $F(k,t)$ is assumed to decay with a relaxation time τ_k.[19] At small wave vectors this k-dependent relaxation mechanism is likely to control *an effective* increase of the sound velocity which we observe for all the alkali elements. In the case of liquid Cs, this *positive dispersion* effect has also been reported in the neutron data of Ref. 2, as well as in the simulation work of Ref. 16. Since an adequate theoretical treatment of the relaxation channels at arbitrary k is not simple, we defer a comprehensive discussion of these features to a subsequent work.[20] For future use in Sec. IV, we only mention that for $k\simeq k_m$ the decay rate $1/\tau_k$ appears to be satisfactory estimated by the Lovesey recipe[21] $1/\tau_k \simeq 2\sqrt{\Delta_k/\pi}$, where the quantity $\Delta_k=(\langle\omega_k^4\rangle/\langle\omega_k^2\rangle)-\langle\omega_k^2\rangle$ is expressed in terms of the second and the fourth frequency moments of $S(k,\omega)$.

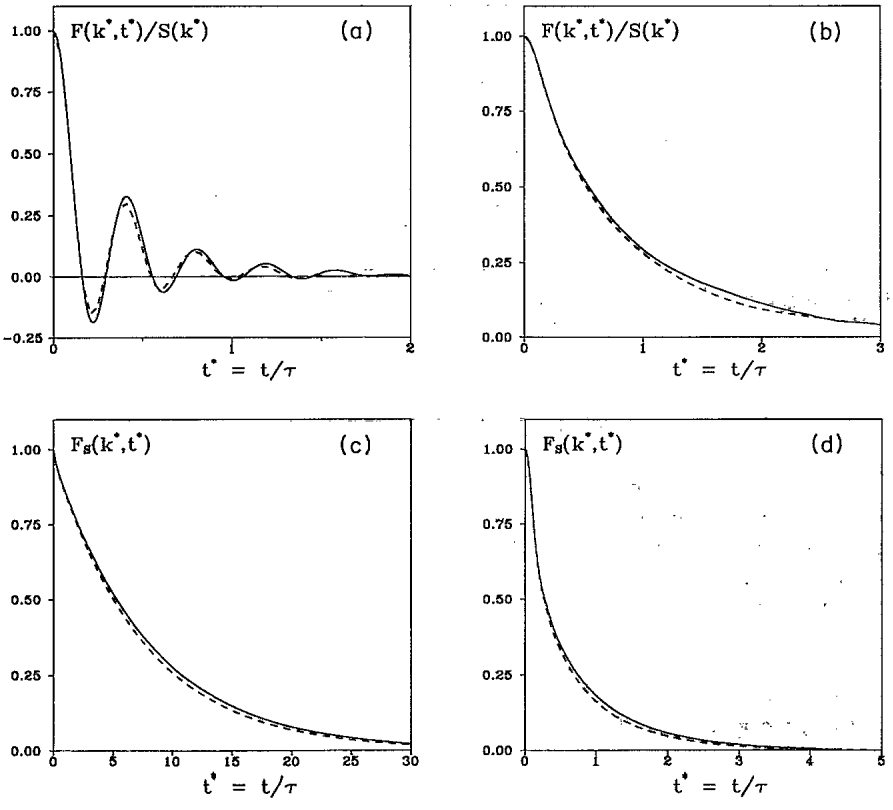

FIG. 5. MD data for the reduced-time dependence of the intermediate scattering functions at two different wave vectors, (a) and (c) $k^*=1.92$ and (b) and (d) 6.86. The solid and the dashed lines are the results for Na and Cs, respectively; for the other elements the results lie in between. In (a) and (b) the full intermediate scattering functions are reported; in (c) and (d) the corresponding self-contributions are reported.

To conclude this section, in Figs. 5(c) and 5(d) we also report our MD findings for the self part of the intermediate scattering function $F_S(k,t)$, at the same wave vectors considered for $F(k,t)$. As is well known, $F_S(k,t)$ decays monotonically at all wave vectors. Physically this time correlation probes single-particle dynamics over different scales of length, ranging from diffusive motion ($k \to 0$) to free-particle behavior at very large wave vectors. Our MD results show that these features can be satisfactorily accounted for by the simple Gaussian approximation

$$F_S(k,t)=\exp[-k^2\delta r^2(t)/6] , \tag{3.1}$$

where $\delta r^2(t)$ is the mean-square displacement of a tagged particle in the liquid. Figures 5(c) and 5(d) clearly show that even in this case the various reduced $F_S(k^*,t^*)$ nearly merge for the different alkalis, as indeed expected at this stage of our analysis.

IV. TRANSPORT COEFFICIENTS

At a macroscopic level the dynamics of a fluid is usually characterized by few transport coefficients, which can be expressed as time integrals of dynamic correlation functions by the well-known Green-Kubo relations. As a result, the values of the transport coefficients are affected by the microscopic time scales ruling the decay of the associated Green-Kubo integrands. Typically, in a dense fluid the time evolution of these integrands is found to be characterized by an initial fast decrease (associated with a decay mechanism provided by "binary" collisions), followed by a long-lasting "tail." A consistent theoretical framework by which both decay mechanisms can be accounted for emerged at the beginning of the 1980s, and combines both kinetic and mode-coupling concepts.[22] Adopting well-justified approximations, recently this general approach has been made of practical use for two transport properties, the diffusion[10] and the shear viscosity[12] coefficients. In the following, we shall summarize the basic ideas behind this simplified approach.

A. The self-diffusion coefficient

The diffusion coefficient D is expressed in terms of the normalized velocity auto-correlation function (VACF) $\psi(t)=\langle \mathbf{v}_1(0)\cdot\mathbf{v}_1(t)\rangle/\langle v_1^2(0)\rangle$ by the Green-Kubo relation

$$D=\frac{k_BT}{M}\int_0^\infty dt\,\psi(t)=\frac{k_BT}{M}\hat{\psi}(z=0) , \tag{4.1}$$

where $\hat{\psi}(z)=\int_0^\infty dt\, e^{-zt}\psi(t)$ denotes the VACF Laplace transform. The dynamical features of the collisional events, affecting the motion of a tagged particle, are better understood introducing the VACF memory function $K(t)$, defined through the Mori equation $\hat{\psi}(z)=[z+\hat{K}(z)]^{-1}$. As a first attempt, we can assume that the only relevant mechanism responsible for the time decay of $K(t)$ is provided from the fast binary decay channel. In such a case the time evolution will be essentially controlled by a single decay time τ_D and can be expressed as $K_B(t)=K_B(0)f(t/\tau_D)$, where B stands for "binary" approximation. The functional form for $K_B(t)$ is not particularly relevant, provided that the memory function decay is sufficiently fast. It is straightforward to show that $K_B(0)=\Omega_0^2$, with

$$\Omega_0^2=\frac{n}{3m}\int d\mathbf{r}\nabla^2 v(r)g(r) \tag{4.2}$$

representing the squared Einstein frequency. Even the decay time $\tau_D=[|\ddot{K}_B(0)|/2K_B(0)]^{-1/2}$ can be evaluated from structural quantities. Indeed after some algebra one finds that ($r_\alpha=x,y,z$)

$$\ddot{K}_B(0)=-\left[\frac{2n}{m}\right]\sum_\alpha\int d\mathbf{r}\left[\frac{\partial^2 v(r)}{\partial x\partial r_\alpha}\right]^2 g(r) - \left[\frac{n}{m}\right]^2\sum_\alpha\int\int d\mathbf{r}\,d\mathbf{r}'\frac{\partial^2 v(r)}{\partial x\partial r_\alpha}\frac{\partial^2 v(r')}{\partial x'\partial r'_\alpha} \times[g^{(3)}(\mathbf{r},\mathbf{r}')-g(r)g(r')] , \tag{4.3}$$

where the second term on the rhs can reliably be evaluated by a superposition approximation for the triple distribution $g^{(3)}(\mathbf{r},\mathbf{r}')$.[10(a)] Therefore, all the relevant quantities ruling the decay of $K_B(t)$ follow from static properties. In our case the reduced values of the quantities Ω_0^2 and τ_D turn out to be $(\Omega_0^*)^2=\Omega_0^2\tau^2\simeq 182.9$ and $\tau_D^*=\tau_D/\tau\simeq 0.092$, with a maximum discrepancy $\simeq 3\%$ between the different alkalis.

The time dependence assumed for the binary memory function leads to a simple expression for the binary diffusion coefficient

$$D_B=c\frac{k_BT}{m\Omega_0^2\tau_D} ; \tag{4.4}$$

where the constant $c\simeq 1$ is slightly dependent on the assumed functional form for f. Choosing, for example, $f(x)=\mathrm{sech}^2 x$ (as in the present paper) the value of c is exactly 1. Equation (4.4) is extremely simple; however, when applied to liquids the value of D_B is found to overestimate substantially the actual diffusion coefficients, as shown in Table II.

The failure of the binary approach clearly indicates that a slowly varying part in $K(t)$ plays a relevant role in dense systems. This tail can be accounted for by a mode-coupling (MC) framework. As a result of the

TABLE II. Diffusion coefficients (in units of 10^{-5} cm^2/s) for the considered liquid alkali metals at the thermodynamic points reported in Table I. D_B and D are the value predicted by the binary [see Eq. (4.4)] and the complete approaches, respectively; D_{MD} is our simulation estimate, and D_{expt} is the experimental value at melting as reported in Refs. 23(a) and 24.

	Na	K	Rb	Cs
D_B	6.30	4.80	3.89	3.34
D [Eq. (4.9)]	4.23	3.77	2.55	2.21
D [Eq. (4.6)]	4.11	3.62	2.46	2.13
D_{MD}	4.06	3.58	2.40	2.11
D_{expt}	4.06–4.35	3.52–3.72	2.60	2.16

theory, the memory function can be written as $K(t)=K_B(t)+K_{MC}(t)$, where the second term is associated with long-lasting behavior. *A priori*, in $K_{MC}(t)$ one should consider all possible bilinear couplings of slow wave-vector-dependent *modes* with the dynamical variable under consideration [in the present case, the fluctuating force entering $K(t)$]. In practice, in the liquid range the only relevant coupling turns out to be with density fluctuations with a wave vector $k \simeq k_m$, which exhibit a marked "de Gennes" slowing down. In such a case, $K_{MC}(t)$ can be written as[10(a)]

$$K_{MC}(t) \simeq C[F_s(k_m,t)-F_0(k_m,t)]\frac{F(k_m,t)}{S(k_m)} . \quad (4.5)$$

Here $C=(k_BT/6nm\pi^2)k_m^4 A$, A denoting the area under the main peak of $h(k)=S(k)-1$ and $F_0(k,t)=\exp(-k_BTk^2t^2/2m)$ represents the free-particle limit, common to both F and F_S. It is easily seen that at short times $K_{MC}(t)$ vanishes as t^4, thus confirming that the initial fast decrease is essentially governed by a binary decay mechanism. In the opposite limit ($t \gg \tau_D$) $K(t) \simeq K_{MC}(t) \propto F_sF$, since in such a time region both $K_B(t)$ and $F_0(t)$ are negligible. Then the diffusion coefficient can be expressed as

$$D=\left[\frac{1}{D_B}+\frac{m}{k_BT}\int_0^\infty dt\, K_{MC}(t)\right]^{-1} , \quad (4.6)$$

where the two distinct contributions arising from $K(t)$ are made apparent. In principle, $K_{MC}(t)$ involves both structural and time-dependent quantities. Its evaluation can, however, be performed by assuming simple approximations for F and F_s. As already noted, in the liquid range a viscoelastic model for $F(k,t)$ works remarkably well for $k \simeq k_m$, where one finds[12]

$$F(k_m,t) \simeq S(k_m)e^{-[B(k_m)/S(k_m)]t} \equiv S(k_m)e^{-\gamma(k_m)t} . \quad (4.7)$$

The quantity $B(k)$ in Eq. (4.7) can easily be expressed by using the aforementioned recipe from Ref. 21. On the other hand, the self-intermediate scattering function is well reproduced by the Gaussian ansatz [Eq. (3.1)]. These approximations yield a considerable simplification, even if in order to obtain the diffusion coefficient from Eq. (4.6) the knowledge of $\delta r^2(t)$ is still required.

However, just this presence of $\delta r^2(t)$ suggest a self-consistent approach to evaluate the diffusion coefficient. In fact, beyond a microscopic short-time region $\delta r^2(t)$ reaches its asymptotic form $6Dt+I$ (I being a small intercept). Substituting in Eqs. (3.1) and (4.5), we easily arrive at a self-consistent set of equations for the diffusion coefficient (4.6) as well as for the intercept I.[10(a)] The values obtained from the diffusion coefficient by such procedure are shown in Table II. The agreement with the simulation result D_{MD} is excellent, the deviations being within 2.5% for all the considered elements. Moreover, the available experimental values for D at melting are also in fair agreement with our simulation findings.

Neglecting the small intercept I, an even simpler perturbative approach can be introduced, which allows one to derive a quite reliable evaluation of D through successive "renormalizations" of the binary result D_B. A first MC correction for D_B is related to the time region where $\delta r^2(t)$ has not yet reached a linear time regime and yields an intermediate diffusion coefficient[10(b)]

$$D_0^{-1} \simeq D_B^{-1}+\left[\frac{k_m^4 A}{6\pi n\Omega_0}\right]e^{-2\pi B(D_B)} , \quad (4.8)$$

where $B(D)=[k_m^2D+\gamma(k_m)]/\Omega_0$. In a second step the mode-coupling effects due to the proper diffusive regime are included leading to the final result

$$D^{-1} \simeq D_0^{-1}+\left[\frac{k_m^4 A}{6\pi^2 n\Omega_0}\right]\frac{e^{-2\pi B(D_0)}}{B(D_0)} . \quad (4.9)$$

Even if this evaluation is less accurate then the previous one (giving a maximum discrepancy about 6%), the simplicity of the formulation is very attractive, since it involves only structural quantities.

As already reported in Ref. 13, the VACF's of the different alkali metals at melting are nearly coincident when expressed as function of the scaled variable $t^*=\tau/t$. Thus, a scaling law is expected to be valid even for the associated transport coefficients. Indeed, from definition (4.1) it is easy to derive an expression for the reduced diffusion coefficient D^*, which reads

$$D=\frac{\sigma^2}{\tau}T^*D^* . \quad (4.10)$$

Note the presence of the reduced temperature $T^*=k_BT/\varepsilon$, which does not follow from simple dimensional arguments. This factor somehow incorporates the small deviations from perfect scaling arising from the slightly different reduced melting temperatures. For the different elements the simulation data yield a value of $D^*_{MD}=0.0354\pm1.7\%$.

B. The shear-viscosity coefficient

The shear-viscosity coefficient η can be expressed as $\eta=\int_0^\infty dt\,\eta(t)$, where $\eta(t)$ is the stress-autocorrelation function (SACF). In a liquid the main contribution to the SACF arises from its potential part

$$\eta_P(t)=\frac{n}{4Nk_BT}\left\langle \sum_{i\neq j}\frac{z_{ij}(0)x_{ij}(0)}{r_{ij}(0)}v'[r_{ij}(0)]\sum_{l\neq m}\frac{z_{lm}(t)x_{lm}(t)}{r_{lm}(t)}v'[r_{lm}(t)]\right\rangle , \quad (4.11)$$

where the summations run over the N particles of the fluid, the combination (zx) is equivalent to (xy) or (yz) because of the spatial isotropy and $v'(r)=dv/dr$. In contrast with D, η is related to collective features. For simplicity, the subscript P will be dropped, keeping in mind that we are always referring to this dominant potential part.

A treatment similar to the one developed for $K(t)$ can also be applied to the SACF.[12] In particular, one extracts binary and mode-coupling contributions by writing $\eta(t)=\eta_B(t)+\eta_{MC}(t)$, where again $\eta_{MC}(t)\propto t^4$ at short times. As before, the rapidly decaying binary part can be characterized by a single decay time τ_η:

$$\eta_B(t)=\eta(0)f(t/\tau_\eta)\ . \tag{4.12}$$

Choosing again the shape function as $f(x)=\mathrm{sech}^2 x$, we deduce a binary viscosity coefficients η_B given by

$$\eta_B=\int_0^\infty dt\ \eta_B(t)=\eta(0)\tau_\eta\ . \tag{4.13}$$

The initial value of the SACF (i.e., the rigidity modulus G) has a dominant potential contribution which can be expressed as

$$G_P=\tfrac{4}{30}\pi n^2\int_0^\infty dr\ r^4\left[v''(r)+4\frac{v'(r)}{r}\right]g(r)\ . \tag{4.14}$$

The short-time behavior of $\eta(t)$ is ruled by the decay time $\tau_\eta=[|\ddot{\eta}(0)|/2G_P]^{-1/2}$, where $\ddot{\eta}(0)$ can be written as the sum of a pair term $\ddot{\eta}^{(2)}(0)$ and of another contribution $\ddot{\eta}^{(3)}(0)$ connected to three-body effects.[12] The explicit expression for the pair term reads

$$\ddot{\eta}^{(2)}(0)=-\frac{n^2}{m}\int d\mathbf{r}\left\{\nabla_r\left[\frac{zxv'(r)}{r}\right]\right\}^2 g(r)\ , \tag{4.15}$$

and is directly evaluable. In the superposition scheme for $g^{(3)}$ and with few other reasonable approximations, $\ddot{\eta}^{(3)}(0)$ can be expressed in terms of the Einstein frequency Ω_0 and reads

$$\ddot{\eta}^{(3)}(0)\simeq-\frac{3}{50}\frac{m\Omega_0^4}{\pi^2\sigma}\int_0^\infty dx\ x^2[S(x)-1]\times[3j_3^2(x)+2j_1^2(x)]\ , \tag{4.16}$$

where $j_l(x)$ denotes the spherical Bessel function of order l. The reduced values of G_P and τ_η for the considered alkali metals are found to be $G_P^*=G_P(\sigma^3/\varepsilon)=16.1\pm4\%$ and $\tau_\eta^*=\tau_\eta/\tau=0.133\pm2\%$. Substituting into Eq. (4.13), one finds that η_B underestimates the simulation findings by nearly 40%. The discrepancy is in the opposite direction to the one found for D, a feature consistent with an approximate Stokes-Einstein relation linking the two coefficients.

Again, the failure of the binary model points out the relevance of additional mode-coupling contributions. The latter can be expressed as[12]

$$\eta_{MC}(t)\simeq\frac{k_BT}{60\pi^2}k_m^4\left\{1-\left[\frac{F_0(k_m,t)}{F_S(k_m,t)}\right]^2\right\}\times\int_{(k_m)}dk\left[\frac{S'(k)}{S(k)}\right]^2\left[\frac{F(k,t)}{S(k)}\right]^2\ . \tag{4.17}$$

The overall time evolution of $\eta_{MC}(t)$ is similar to the one already discussed for $K_{MC}(t)$, with two noteworthy differences. The first one concerns the MC relaxation channel, which is now ruled by F^2 (rather than F_SF) as a consequence of the collective nature of the SACF. Second, the presence of $[S'(k)]^2$ in the MC vertex implies that the main contribution to the integral is provided by wave vectors k slightly away from k_m. This means a comparatively less marked de Gennes slowing down, and a consequently faster decay of $\eta_{MC}(t)$.

A preliminary test of the theory can be performed adopting for F_S and F the aforementioned approximations and using the MD data for the mean-square displacement $\delta r^2(t)$. Being now confident in the scaling hypothesis, we adopt a reduced SACF $\eta(t^*)$ to represent our class of systems and report in Fig. 6 the comparison between theoretical and simulation findings. Although there is a slight tendency to underestimate the MD data, the overall agreement appears to be quite satisfactory.

An evaluation of η, avoiding any resort to MD results, is possible adopting the Vineyard approximation $F_S(k,t)\simeq F(k,t)/S(k)$. The mode-coupling contribution to the shear viscosity can be now written as

$$(\eta_{MC})_V\simeq\frac{k_BT}{30\pi^2A}\sqrt{2\pi}[S(k_m)-1]k_m^4\alpha\times\left[\frac{S_\pm}{2B(k_m)}-\frac{1}{2k_m}\left[\frac{\pi m}{k_BT}\right]^{1/2}\right] \tag{4.18}$$

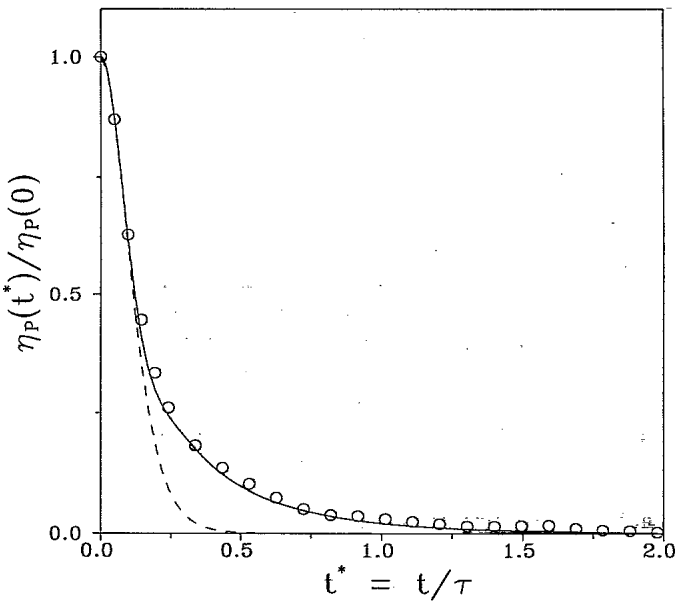

FIG. 6. Stress-autocorrelation function in reduced-time units. The dashed and the solid lines represent the predictions of the binary and the full theories, respectively. The open circles are our MD data.

TABLE III. Shear-viscosity coefficients (in units of mp) for the considered liquid alkali metals at the thermodynamic points reported in Table I. η_B and η are the values predicted by the binary and full theories, respectively. η_{MD} is our simulation finding, and η_{expt} is the experimental value as reported in Refs. 23(b) and 24. The subscript P refers to the potential part of the shear-viscosity coefficient.

	Na	K	Rb	Cs
$(\eta_B)_P$	3.02	2.45	3.10	3.23
$(\eta)_P$	4.89	4.15	5.33	5.40
$(\eta_{MD})_P$	5.22	4.50	5.84	6.07
η_{MD}	5.30	4.60	5.95	6.16
η_{expt}	6.68	5.14–5.25	5.52–6.44	6.50

with the notations

$$S_{\pm}=1+[S(k_m)-1]e^{-x_{\pm}^2/2}$$

and

$$x_{\pm}^2 \simeq \frac{1+2[S(k_m)-1]/e}{1+[S(k_m)-1]/2e} .$$

Moreover, the dimensionless quantity α depends on the value of $S(k_m)$.[12] The values deduced for $(\eta_{MC})_V$ agree quite closely with those obtained from the direct time integration of Eq. (4.17). Considering the approximations necessary for this collective case, the final theoretical results $\eta=\eta_B+\eta_{MC}$ compare rather well with the simulation findings. Table III indicates the quality of the comparison between theory, simulation, and the available experimental data. In view of the several uncertainty factors present in all these data, the overall agreement is to be considered satisfactory, with the possible exception of liquid Na.

A scaling law can be introduced here too, leading to a reduced shear-viscosity coefficient η^* defined through the relation

$$\eta=\frac{1}{T^*}\left[\frac{\varepsilon\tau}{\sigma^3}\right]\eta^* . \tag{4.19}$$

The reduced temperature arises in Eq. (4.19) from the initial definition (4.11) of the SACF. η^* presents a value almost identical for all the alkali metals at melting, namely, $\eta^*=3.245\pm0.4\%$. As a final remark, we may introduce a sort of reduced Stokes-Einstein relationship

$$D^*\eta^*=\frac{T^*}{4\pi f} , \tag{4.20}$$

where the dimensionless quantity f is such that $f\sigma$ is a measure of an effective dynamical radius of the particles. Our data indicate that $f\simeq0.61$ for all the alkali metals under consideration.

V. CONCLUDING REMARKS

A first important result of the present work is the possibility of a unitary description of the liquid state properties of the "classical" alkali metals near the melting point. In this respect, our analysis gives sound support to earlier attempts to finding a common behavior for all these systems. The reliability of this conclusion is based on a comprehensive study of both structural and time-dependent properties by a molecular-dynamics simulation. Moreover, we have benefited from the availability of new accurate experimental data.

In our computer simulations, for the alkalis we have adopted the potential model implemented several years ago by Price, Singwi, and Tosi. Although not expressible in a simple analytic form, this effective pair interaction potential turns out to provide a quite satisfactory description of the properties of the real systems. In particular, the favorable comparison obtained in Sec. III between our data and the experimental $S(k,\omega)$ for liquid Cs supplements earlier similar findings for liquid Rb, and indicates that the potential model is sufficiently realistic. Quantitatively, the potential is also found to "scale" to a good approximation for the various elements, giving a convenient starting point for ascertaining their common features.

The second relevant aspect of our analysis deals with two important nonequilibrium quantities, the diffusion and shear-viscosity coefficients. Our simulation data for the associated Green-Kubo integrands are found to confirm the validity of the simplified mode-coupling theories which have been developed in the last few years. In particular, the existence of two well-separated "relaxation channels" for the appropriate dynamic correlations is given a sound physical basis. Finally, the evaluation of the transport coefficients themselves offers a possibility of an overall comparison among theory, simulation and experiments. The result of such a comparison appears to be satisfactory, confirming all the aforementioned conclusions.

ACKNOWLEDGMENTS

The authors are grateful to C. Morkel for providing unpublished neutron data on liquid Cs, and to R. D. Mountain and S. K. Lai for useful correspondence. Computer simulations were performed under a convention between Consiglio Nazionale delle Ricerche and Centro di Calcolo Elettronico dell'Italia Nord-Orientale.

[1]N. H. March, *Liquid Metals* (Cambridge University Press, Cambridge, 1990).
[2]T. Bodensteiner, C. Morkel, P. Müller, and W. Glaser, J. Non-Cryst. Solids, **117-118**, 941 (1990); C. Morkel and T. Bodensteiner, J. Phys: Condens. Matter **2**, 251 (1990).
[3]J. R. D. Copley and J. M. Rowe, Phys. Rev. A **9**, 1656 (1974).
[4]R. D. Mountain, Inst. Phys. Conf. Ser. **30**, 62 (1977).
[5]M. J. Huijben and W. van der Lugt, Acta Crystallogr. A **35**, 431 (1979).
[6]H. B. Singh and A. Holz, Phys. Rev. A **28**, 1108 (1983).
[7]N. Matsuda, H. Mori, K. Hoshino, and M. Watabe, J. Phys.: Condens. Matter **3**, 827 (1991).

[8]D. L. Price, K. S. Singwi, and M. P. Tosi, Phys. Rev. B **2**, 2983 (1970).

[9]For a review see A. Sjölaner, in *Amorphous and Liquid Materials,* edited by E. Lüscher, G. Fritsch, and G. Jacucci (Martinus Nijhoff, Dordrecht, 1987), p. 239.

[10](a) U. Balucani, R. Vallauri, T. Gaskell, and S. F. Duffy, J. Phys: Condens. Matter **2**, 5015 (1990); (b) U. Balucani, S. F. Duffy, and R. Vallauri, in *Recent Developments in the Physics of Fluids,* Proceedings of the International Symposium (IOP, Oxford, 1992), Sec. 2.

[11]U. Balucani and R. Vallauri, Phys. Rev. A **40**, 2796 (1989).

[12]U. Balucani, Mol. Phys. **71**, 123 (1990).

[13]U. Balucani, A. Torcini, and R. Vallauri, Phys. Rev. A **46**, 2159 (1992).

[14]U. Balucani, R. Vallauri, and T. Gaskell, Phys. Rev. A **37**, 3386 (1988).

[15]A. Rahman, Phys. Rev. A **9**, 1667 (1974).

[16]S. Kambayashi and G. Kahl, Europhys. Lett. **18**, 421 (1992).

[17]W. van der Lugt and B. P. Alblas, in *Handbook of Thermodynamic and Transport Properties of Alkali Metals,* edited by R. W. Ohse (Blackwell Scientific, Oxford, 1985), p. 299.

[18]J. W. E. Lewis and S. W. Lovesey, J. Phys. C **10**, 3221 (1977).

[19]J. P. Boon and S. Yip, *Molecular Hydrodynamics* (McGraw-Hill, New York, 1980).

[20]U. Balucani, G. Ruocco, A. Torcini, and R. Vallauri, Phys. Rev. E (to be published).

[21]S. W. Lovesey, J. Phys. C **6**, 1856 (1973).

[22]L. Sjögren and A. Sjölander, J. Phys. C **12**, 4369 (1979); L. Sjögren, *ibid.* **13**, 705 (1980).

[23](a) M. Gerl and A. Bruson, *Handbook of Thermodynamic and Transport Properties of Alkali Metals* (Ref. 17), p. 843; (b) E. E. Shpil'rain, K. A. Yakimovich, V. A. Fomin, S. N. Skovorodjko, and A. G. Mozgovoi, *ibid.*, p. 753.

[24]*Transportphänomene I,* edited by K. Schäfer, Landolt-Börstein, Zahlenwerte und Funktionen aus Physik, Chemie, Astronomie, Geophysik und Technik, Pt. 5a (Springer-Verlag, Berlin, 1969).